SCIENCE CHINA
Technological Sciences

Special Topic: Advanced Rare Earth Science and Technology
•Review•

September 2018 Vol.61 No.9: 1301–1308
https://doi.org/10.1007/s11431-018-9311-x

Revisit of energy transfer upconversion luminescence dynamics —the role of energy migration

TU LangPing[1,2], ZUO Jing[1] & ZHANG Hong[1,2*]

[1]*Van't Hoff Institute for Molecular Sciences, University of Amsterdam, Amsterdam 1098 XH, The Netherlands;*
[2]*Changchun Institute of Optics, Fine Mechanics and Physics, Chinese Academy of Sciences, Changchun 130033, China*

Received March 2, 2018; accepted June 19, 2018; published online August 9, 2018

Upconversion is a process in which one photon is emitted upon absorption of several photons of lower energy. Potential applications include super resolution spectroscopy, high density data storage, anti-counterfeiting and biological imaging and photo-induced therapy. Upconversion luminescence dynamics has long been believed to be determined solely by the emitting ions and their interactions with neighboring sensitizing ions. Recent research shows that this does not hold for nanostructures. The luminescence time behavior in the nanomaterials is confirmed seriously affected by the migration process of the excitation energy. This new fundamental insight is significant for the design of functional upconversion nanostructures. In this paper we review relevant theoretical and spectroscopic results and demonstrate how to tune the rise and decay profile of upconversion luminescence based on energy migration path modulation.

rare earth, upconversion, energy migration, luminescence dynamics

Citation: Tu L P, Zuo J, Zhang H. Revisit of energy transfer upconversion luminescence dynamics—the role of energy migration. Sci China Tech Sci, 2018, 61: 1301–1308, https://doi.org/10.1007/s11431-018-9311-x

1 Introduction

Lanthanide (Ln) ions doped upconversion (UC) materials have unique property of converting lower energy (long wavelength) photons to higher energy (short wavelength) photons, which is believed to realize via sequential absorption and/or energy transfer processes. This property has great potential applications in broad fields, e.g. display, biology, anti-counterfeiting, and solar cell, etc [1,2]. Although the excitation density of realizing observable UC in these materials is orders of magnitude lower than that of coherent sum-frequency generation, the UC efficiency is only several percent in a macroscopic crystal under 980 nm excitation at excitation density less than 100 W/cm^2. For nanometer sized materials, the efficiency is even lower [3].

To improve the UC efficiency, a comprehensive understanding of UC luminescence dynamics is a must. However, for the most efficient UC mechanism—energy transfer upconversion (ETU), the relevant luminescence dynamics is still not well disentangled due to the fact that the UC emission involves complex interactions between multiple excited Ln^{3+} ions.

From experiments on UC dynamics it is observed that (i) the "lifetimes" of UC emission are normally much longer than the intrinsic lifetimes of emissive energy levels; (ii) the emission based on ETU has usually a rising component of the time evolution. These results are difficult to understand from the existing UC picture. It is assumed that continuous energy transfer processes from long-lived sensitizers (e.g. Yb^{3+}) to activators (e.g. Er^{3+}, Tm^{3+}, Ho^{3+}) may play a role here, which is, however, lack of evidence and a clear picture till now. In recent years, with the advance of nanotechnology, precisely engineered material structures on nanometer scale are becoming possible. Combination of (i) well-tailored na-

*Correspondence author (email: H.Zhang@uva.nl)

nostructures, (ii) specifically designed nonlinear spectroscopic experiments and (iii) careful theoretical modeling have allowed us to have an unprecedented clear vision of the UC luminescence dynamics in nanostructures. In particular, non-neglectable sensitizer-to-sensitizer energy migration effect (e.g. $Yb^{3+} \rightarrow Yb^{3+}$) on UC dynamics is confirmed both in theory and experiment [4]. Based on this new fundamental insight, a fine control of UC dynamics trace (either the rise or decay process) is achieved by tuning the energy migration paths in specifically designed nanostructures. The deeper understanding also paves the way for application-optimized design of novel functional UC nanostructures and even to improve the UC emission efficiency. In the following we will focus on our recent work on this topic.

2 Traditional understanding of the UC dynamics

Conventionally, energy transfer mechanism dominant UC process is usually simplified to monomer to monomer (e.g. sensitizer to activator) sequential interactions (as indicated in Figure 1), where the energy migration between sensitizers is treated as infinitely fast (Inokuti-Hirayama model) [5].

In that case, the UC dynamics could be described by a series of differential equations, taking into account only the population and depopulation processes between different energy levels, and ignoring the multi-step energy migration processes between all identical energy levels. The simplified rate equations could be described as [6]:

$$\begin{aligned}\frac{\mathrm{d}N_i}{\mathrm{d}t} &= \sum \text{population rate} - \sum \text{depopulation rate} \\ &= \sum_j \left(N_j A_{ji}^{ED} - N_i A_{ij}^{ED}\right) + \sum_j \left(N_j A_{ji}^{MD} - N_i A_{ij}^{MD}\right) \\ &\quad + \left(N_{i+1} W_{i+1,i}^{NR} - N_i W_{i,i-1}^{NR}\right) \\ &\quad + \sum_{ij,kl} \left(N_j N_l C_{ji,lk}^{ET} - N_i N_k C_{ij,kl}^{ET}\right),\end{aligned}$$

where N_i is the population density of each energy level, A_{ij}^{ED} and A_{ij}^{MD} are the Einstein coefficients for electric dipole (ED) and magnetic dipole (MD) radiative transitions from energy level i to j. $W_{i+1,i}^{NR}$ is the nonradiative multiphonon relaxation (NMPR) rate constant from energy level i+1 to i. $C_{ij,kl}^{ET}$ is the microscopic energy transfer parameter for the transfer of energy via the sensitizer i to j transition and the activator k to l transition. The coefficients ED, MD and $C_{ij,kl}^{ET}$ can be calculated by Judd-Ofelt theory, while the NMPR rate is treated with a modified energy gap law, and a related description of phonons is used to calculate phonon-assisted ET constants. Finally, the intensity of any given UC emission is proportional to the product of the corresponding N_i of each energy level and its radiative transition rates.

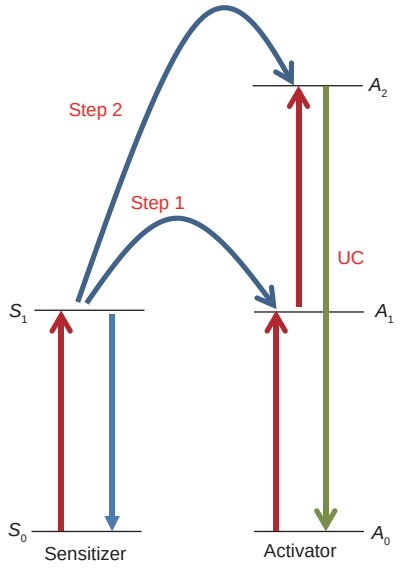

Figure 1 (Color online) Schematic diagram of ETU mechanism which based on the sensitizer to activator sequential energy transfer.

Although the above mentioned approach (simultaneous rate equations) is most commonly used in analyzing the UC dynamics, there are still some drawbacks that cannot be ignored: (i) it treats all the identical ions equally. Therefore all the influence induced by the ions distribution is not taken into consideration. This impact is, however, very important for UC properties in heterogeneous nanostructure; (ii) it remains a challenge to get an accurate solution due to the difficulty in determining all the rate constants in these complex rate equations, as reflected in the fact that the theoretical predictions out of the rate equations usually do not fit well the experimental results. Taking the simplest UC system as an example (i.e. sensitizer with two energy levels and activator with three energy levels, as indicated in Figure 1), it is easy to find that the UC decay lifetime should be a half of the sensitizers lifetime, which, however, is not conformed by the facts; (iii) this method offers only limited guidance for further improving UC efficiency since it provides merely statistical average results, and lacks the relevant microscopic nature of the UC process.

In the past few decades, some modified dynamic models have been proposed. For example, the models suggested by Zusman-Burshtein and Yokota-Tanimoto take into account the energy migration effect between sensitizers [7,8]. The Zusman-Burshtein model was used to treat energy migration as a series of excited states "hopping" processes [7]. It fits better the situation that the sensitizer-sensitizer interaction is much stronger than the sensitizer-activator one. Whereas the Yokota-Tanimoto model employed a diffusion constant and a classical diffusion formalism to quantify the energy migration dynamics, which is more appropriate to the relatively

weak energy migration processes [8]. On the other hand, Grant [9] introduces time-dependent energy transfer rates into the rate equations. Despite all these efforts, a comprehensive understanding of UC dynamics remains a challenge, due to (i) these modified models are difficult to deal with energy migration process in heterogeneous systems (such as core/shell nanostructures), and (ii) they are designed for the linear luminescence, not appropriate for the non-linear UC emission which involves interactions between multiple excited states [10].

3 New insight of the UC dynamics—the key role of energy migration effect

As mentioned above, the common limitation of previous models is the incapability to deal with the energy migration process properly. In our opinion, this shortcoming is primarily due to their unwise choice of the material system. In the early time, sensitizers and activators are always co-doped in the materials. the energy migration processes between sensitizers are inevitably interrupted by energy transfer processes between sensitizers and activators. In that case, the migration effects are difficult to be evaluated. This dilemma can be solved by utilizing a specially designed nanosystem which we named as "dopant ions spatial separated" (DISS) nanostructure [4, 11]. The DISS nanostructures with separated sensitizer and activator regions (such as core@shell@shell nanostructures) have already been intensively studied with focus on the verification/investigation of steady-state energy migration effect [11–16]. In our recent work, by locating sensitizers and activators into different regions of one single nanoparticle, DISS nanostructure has the capability to separate all the three basic UC processes, i.e. light absorption, energy transition/migration and UC emission processes, from each other as indicated in Figure 2. Consequently, the energy migration effect can be clearly analyzed by (i) varying the migration layer thickness or (ii) changing the doping concentration of the carrier ions in the migration layer.

The other issue is that the traditional analytical approach (such as simultaneous rate equations) is helpless to describe properly the actual energy migration processes since it treats all the identical ions equally. This issue can be addressed by introducing a sublattice-based Monte Carlo simulation approach, which is able to build a reliable connection between macroscopic UC phenomena and microscopic multiple ion-to-ion interactions [4]. As shown in Figure 3, UC emission can be regarded as being induced by two or more randomly walked excited states "colliding" on one activator ion from the microscopic point of view. Therefore, in an ideal situation in which, if we can track the time-dependent behaviors of all the excited ions in one nanoparticle, the macroscopic

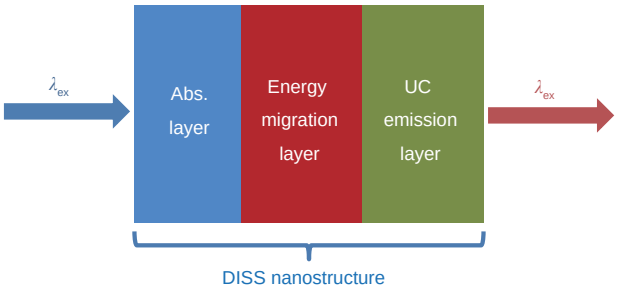

Figure 2 (Color online) Schematic diagram of the UC processes in "dopant ions spatial separated" nanostructure, in which the three basic processes: photon absorption, energy migration and UC emission are spatially separated in one nanoparticle.

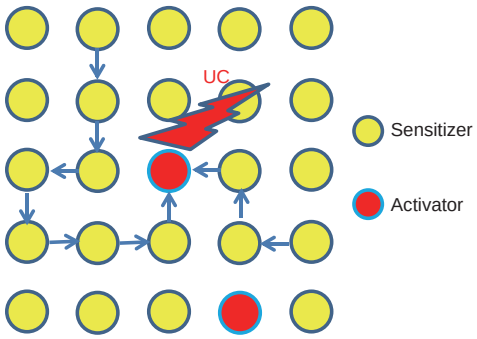

Figure 3 (Color online) Schematic diagram of the microscopic picture of UC emission which is induced by the "collision" of the two or more randomly walking excited states.

UC phenomena could be rebuilt by mapping all the microscopic dynamical processes. In contrast to previously reported models of UC phenomena related to Monte Carlo simulation or DFT (density function theory) calculation [16–22], the model proposed by reference [4] Zhang et al. [4] includes three significant features: (1) it not only simulates the energy migration process, but also contains the light absorption and UC emission processes. Thus it offers a clear microscopic vision of entire UC process from light absorption to UC emission. (2) It is particularly advantageous in dealing with the situation of complicated nanosystems, such as studying the energy migration on the core-shell interface of heterogeneous structures. (3) By introducing time evolution process into the system, it can not only be applied for the steady-state simulation, but also for dealing with UC dynamics.

3.1 Construction of Monte Carlo simulation model for UC dynamics

The good news for constructing the Monte Carlo simulation model of UC process is that most of the microscopic interaction parameters can be reasonable obtained from experiments or quantum mechanical calculation. The construction process is described in detail in our previous report [4]. Here,

several basic ideas are listed to help a better understanding of this model.

(i) The crystal structure of nanoparticle is simplified to a simple cubic structure which only contains sensitizers and activators. Taking $NaYF_4$: 20% Yb, 2% Er nanoparticle as an example, which contains 20% sensitizer and 2% activator, respectively. According to the Ln^{3+} doping concentration and the lattice parameters of hexagonal phase $NaYF_4$ matrix, the distance between the nearest neighboring ions is calculated to about 0.8 nm. Therefore, a 20 nm diameter nanoparticle is modeled as a 25×25×25 cube sublattice, which consists 15625 grid points, and each grid point is randomly set as one sensitizer or activator ion with the ratio of 10 to 1.

(ii) The energy states of Ln^{3+} ions take the simplest situation: sensitizer ions have two energy levels (labeled as S_1 and S_0, respectively) and activator ions have three energy levels (labeled as A_2, A_1 and A_0, respectively), as shown in Figure 1. Furthermore, due to the relatively small effects, some secondary processes are reasonably ignored without affecting the basic understanding of the model, including: stimulated emission, cross relaxation ($A_2+S_0 \rightarrow A_1+S_1$) and excited states absorption ($A_1+h \rightarrow A_2$) processes, etc.

(iii) For the simulation parameters (as placed in Table 1).

a) The recombination rate of S_1, $A_1$and A_2 states are obtained from the reciprocal of the measured lifetime of each energy states (i.e. ~1 ms lifetime for S_1, A_1 states, and ~ 140 μs lifetime for A_2 state, all evaluated from the nature of Yb^{3+} and Er^{3+} ions).

b) The absorption cross section of S_0 and A_0 are referred to the properties of Yb^{3+} and Er^{3+}, respectively [23].

c) The quantum yield of A_2 state (i.e. 50%) is evaluated from the generally luminescence efficiency of lanthanide ions doped phosphors. The surface quenching rate is determined to ~10^5 s^{-1} in the $NaYF_4$: 20% Yb, 2% Er bare core nanoparticle, which is mutually authenticated by ① the UC efficiency of bare core nanoparticle and ② the experimental and simulation results of particle size dependent UC emission. The details are discussed in our previous report [4].

Table 1 The simulation parameters of UC processes, which is calculated from β-$NaYF_4$: 20%Yb, 2% Er crystal

Parameters	Value
Recombination rate of S_1	10^3 s^{-1}
Recombination rate of A_1	10^3 s^{-1}
Recombination rate of A_2	7×10^3 s^{-1}
Energy migration rate of $S_1 \rightarrow S_0$	10^5 s^{-1}
Energy transfer rate of $S_1 \rightarrow A_0$	2.5×10^4 s^{-1}
Energy transfer rate of $S_1 \rightarrow A_1$	3.2×10^3 s^{-1}
Energy transfer rate of $A_1 \rightarrow S_0$	1.0×10^4 s^{-1}
Energy migration rate of $A_1 \rightarrow A_0$	5×10^3 s^{-1}
Energy transfer rate of $A_1 \rightarrow A_1$	600 s^{-1}
Absorption cross section of S_0	1.17×10^{-20} cm^2
Absorption cross section of A_0	1.7×10^{-21} cm^2
Surface quenching rate	10^5 s^{-1}
Quantum yield of A_2 state	50%

d) Based on the assumption that the energy transfer/migration processes only occur between the two closest neighboring ions, the energy transfer/migration probability can be considered as the sum up of three parts:

$$P = \frac{\left(\frac{R_0}{R}\right)^s}{\tau_s} \quad (s = 6, 8, 10). \tag{2}$$

1) s=6 for dipole-dipole interactions (P_{dd}); 2) s=8 for dipole-quadrupole interactions (P_{dq}); 3) s=10 for quadrupole-quadrupole interaction(P_{qq}). τ_s is the actual lifetime of the donor excited states, R_0 is the critical transfer distance for which excitation transfer and spontaneous deactivation of the sensitizer have equal probability. R is the real distance between the two ions. For the β-$NaYF_4$: 20%Yb, 2% Er nanoparticle where the Yb^{3+}-to-Yb^{3+} distance R is fixed to ~ 0.8 nm, the three relevant interaction parameters are calculated to: P_{dd}~2.8×10^4 s^{-1}, P_{dq}~3.0×10^4 s^{-1} and P_{qq}~ 6.4×10^4 s^{-1}. Therefore, the $Yb^{3+} \rightarrow Yb^{3+}$ energy migration rate is calculated to ~10^5 s^{-1}.

On the basis of these fixed parameters, the time evolution of macroscopic UC phenomenon can be divided into a series of microscopic events in successive time steps (Δt: 1 μs). Each time step accompanied by all the possible excited state generation or depletion for every ion. And random numbers are generated by computer to decide which events actually occur in this step. After each step, the microscopic distribution of excited states was updated to reflect the new energy configuration of the nanoparticle.

3.2 Some microscopic physical pictures of UC phenomena — established by Monte Carlo simulation

Utilizing the Monte Carlo simulation approach, we can obtain some meaningful microscopic physical pictures of the macroscopic UC phenomena.

(i) The UC emission efficiency.

For a single Ln^{3+} ions, its microscopic probability of being excited by the pump within one time step can be calculated as:

$$P_{abs} = \rho \frac{\sigma \Delta t}{E_{h\nu}}, \tag{3}$$

where ρ is the excitation power density, σ is the absorption cross section of Ln^{3+} ion, $E_{h\nu}$ is the energy of one excitation photon and Δt is the time step (for example: 1 μs). If we assume ρ is 100 W/cm^2, σ is 1.17×10^{-20} cm^2 (referred as the Yb^{3+} ions), and the excitation wavelength is 980 nm, the value of P_{abs} is then calculated as low as 5.76×10^{-6}. Therefore, taking the $NaYF_4$: 20% Yb 2% Er (20 nm) @$NaYF_4$

Table 2 The simulation results for $NaYF_4$: 20% Yb 2% Er (20 nm) @$NaYF_4$ core/shell and $NaYF_4$: 20% Yb 2% Er (20 nm) bare core nanostructures (simulation time period: 2 s)

Parameters	Core/shell	Bare core
Absorbed photons	166505	166505
Quenched by surface	0	141075
Recombined on the S_1 state	130249	20516
Recombined on the A_1 state	31132	4744
Recombined on the A_2 state	2515	79
UC emission photons	1260	42
UC efficiency	0.75%	0.03%
Excited states number	~85	~15

core/shell nanoparticle as an example. As shown in Table 2, despite one single nanoparticle contains ~1.4×10^4 Yb^{3+} sensitizer ions, furthermore, taking the long lifetime of Yb^{3+} excited state (around 1 ms, about 1000 time step) into account, only dozens of (~85) Yb^{3+} ions could be excited simultaneously under the steady-state condition (ρ is 100 W/cm^2), due to the weak pump absorption ability of Yb^{3+} ions. In other words, the probability of Ln^{3+} ions being excited is less than 1% (under the condition of pump excitation of 100 W/cm^2). Therefore the "collision" of randomly walked excited states is relatively difficult, and most of the absorbed energy (~97%) will be consumed through the sensitizer/activator recombination process during the random walk period of excited states. Thus it leads to a relatively low UC efficiency (0.75±0.1%). Furthermore, if we take the surface quenching effect into account, for the $NaYF_4$: 20% Yb 2% Er bare core nanostructure with 20 nm diameter, ~85% excited states will be eliminated by the surface quenching sites, thus further decreaseing the UC efficiency to 0.03±0.01%. All these simulated results are well in line with the experimental reports [3].

(ii) The non-linear relationship between laser power (P) and UC intensity (I).

The non-linear p-I relationship ($I=p^n$, $n>1$) is regarded as a feature of UC emission process, which can also be well simulated by our model. Obviously, increasing the number of excited states in a confined space, will nonlinearly increase the "collision" possibility of excited states. For a two-photon processes, the simulated n value is 1.97 [4], almost equal to the ideal theoretical value (n=2) [24].

(iii) The $Yb^{3+}\rightarrow Yb^{3+}$ energy migration dynamics.

With the utilization of Monte Carlo simulation, we can understand the $Yb^{3+}\rightarrow Yb^{3+}$ energy migration dynamics from a unique angle.

In the traditional understanding, since the energy migration effect is not taken into consideration, the lifetime of Yb^{3+} excited states (e.g. 1 ms) is regarded as the average time of

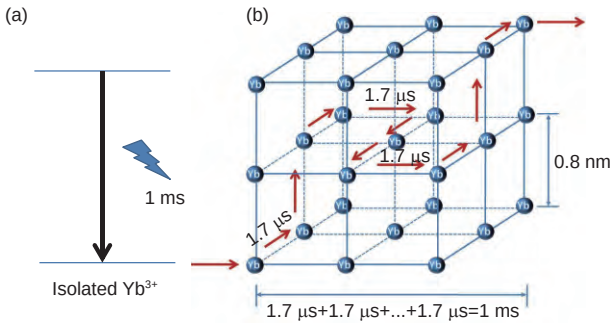

Figure 4 (Color online) The microscopic picture of excited states dynamics for (a) isolated Yb^{3+} ion, and (b) energy-migrated Yb^{3+} in the $NaYF_4$: 20% Yb sublattice.

excited state staying at one isolated Yb^{3+} ion (Figure 4(a)). It can be calculated by the equation:

$$\tau = \frac{1}{I_0}\int_0^\infty I(t)\mathrm{d}t, \tag{4}$$

where $I(t)$ and I_0 are the luminescence intensity as a function of time t and the maximum emission intensity, respectively.

However, utilizing the simulation approach, we find that due to the efficient energy migration (in $NaYF_4$: 20% Yb sublattice, $Yb^{3+}\rightarrow Yb^{3+}$ energy migration rate is two orders of magnitude higher than Yb^{3+} self-recombination rate), Yb^{3+} excited states tend to migrate among hundreds of Yb^{3+} ions before relaxing to its ground state. Therefore, despite the excited state lifetime will not be affected by energy migration, the time spent on each migrated ion is correspondingly reduced to around 1.7 μs (Figure 4(b)). Furthermore, if we add energy traps (either activator or energy quenching site) into the sublattice to cut off the energy migration path, obviously, the average "lifetime" of Yb^{3+} excited states, as well as the UC emission dynamics will be influenced by the number and location of traps. Guided by this understanding, in the following section, we efficiently control the UC dynamics by tailoring the ions distribution in "dopant ions spatial separated" nanostructures. The details of the relevant results can be found in our previous report [4].

3.3 Tailoring UC dynamics via DISS nanostructures

Firstly, we prepared a core/shell/shell DISS nanostructure: YbEr@Yb@YbNd (short for $NaYF_4$: 20% Yb, 2% Er @$NaYF_4$: 20% Yb @$NaYF_4$: 10% Nd, 20%Yb nanoparticle, the size of core and each shell were verified to ~25.0 nm, ~2.8 nm, ~3.0 nm, respectively). To specifically study the relationship between energy migration process and UC dynamics, a binary pulse excitation setup was built, in which the time gap (Δt) between a 800 nm and a 980 nm nanosecond pulse is tunable from –200 μs to 1000 μs (Figure 5(a)). As indicated in Figure 5(b), 980 nm laser excites sensitizer Yb^{3+} all over the whole nanoparticle, whereas 800 nm only excites another sensitizer (Nd^{3+}) only located in the outer

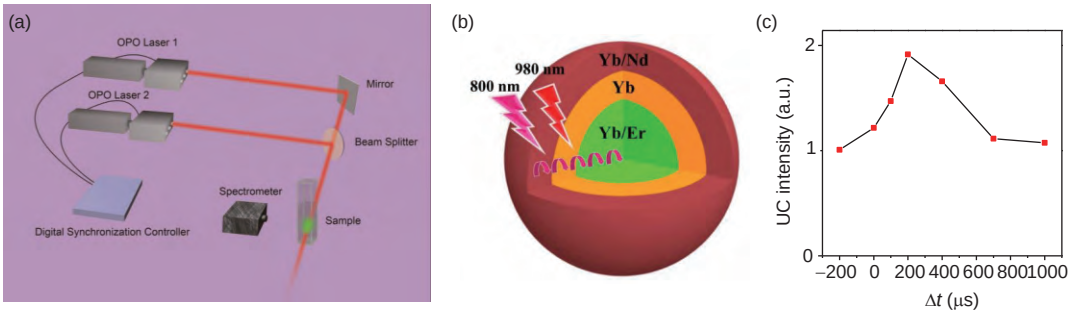

Figure 5 (Color online) (a) Schematic diagram of the experimental setup for binary pulsed (800 nm and 980 nm) excitation; (b) the YbEr@Yb@YbNd DISS nanostructure used in the binary pulsed excitation experiment; (c) time gap dependent UC emission intensity of the YbEr@Yb@YbNd nanoparticles (integrated from 500 nm to 700 nm).

layer. Therefore, the energy obtained from 800 nm excitation has to migrate longer distance (via $Nd^{3+}\rightarrow Yb^{3+}$ energy transfer in the outer layer and $Yb^{3+}\rightarrow Yb^{3+}$ energy migration in the middle layer) to achieve the UC emission of Er^{3+}.

In such a case, a good visualization of the evidence for energy migration temporal effect could be obtained by measuring the time gap dependent binary pulsed co-excited UC emission intensity of the nanoparticle. Strikingly, according to our observation, the strongest UC luminescence occurs not at the moment Δt=0, but when the 980 nm pulse is ~200 μs later than 800 nm pulse (Figure 5(c)). Since the $Nd^{3+}\rightarrow Yb^{3+}$ energy transfer is only ~20 μs [25], fast enough to be neglected, the ~200 μs time gap mainly corresponds to the extra $Yb^{3+}\rightarrow Yb^{3+}$ energy migration time in the middle layer. The significance of the results are: (1) it is the first time that the energy migration dynamics has been directly observed in real time, and (2) it confirms that the energy migration temporal effect is non-negligible. According to our simulation results, in $NaYF_4$: 20% Yb sublattice, despite each step of $Yb^{3+}\rightarrow Yb^{3+}$ energy migration only consumes ~1.7 μs (as shown in Figure 4), and even if the migration distance is just a few nanometers, the time delay for UC will still be accumulated to several hundred microseconds due to (1) the randomly walking nature of energy migration, and (2) the non-linear property of UC emission. Guided by this understanding, two types of DISS nanostructure are designed to tune the rise and decay edges of UC dynamics respectively.

To quantitatively tune the rise edge of the time trace of UC emission, DISS nanostructure characterized with spatially separated absorption (sensitizer) and emission (activator) regions is suggested. Taking the above mentioned YbEr@Yb@YbNd nanostructure as an example. As shown in Figure 6, under 800 nm excitation, UC emission of this structure relies fully on the $Yb^{3+}\rightarrow Yb^{3+}$ energy transfer to transport the absorbed energy from the outer layer (Nd^{3+}) to the core area (Er^{3+}). According to our simulation, due to the non-neglectable $Yb^{3+}\rightarrow Yb^{3+}$ energy migration time (~1.7 μs per step), the required time of Er^{3+} receiving the migrated energy can be well controlled by the middle layer thickness, appearing

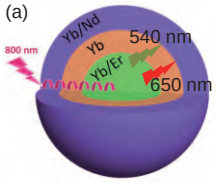

Middle layer thickness	540 nm Rise time (μs)	650 nm Rise time (μs)
0 nm	200	370
3 nm	426	596
5 nm	564	765

Figure 6 (Color online) (a) Schematic illumination of the UC process in the $NaYF_4$: 20% Yb, 2% Er @$NaYF_4$: 20% Yb @$NaYF_4$: 10% Nd, 20%Yb core/shell/shell DISS nanostructure under 800 nm excitation. (b) The tunable rise edges (tailored by varying the middle layer thickness) of the UC emission time traces of DISS nanostructures (nanoparticles excited by 10 nanoseconds 800 nm pulse).

as a tunable rise edge of UC luminescence time trace. Indeed, according to the experimental results, increasing the middle layer thickness from 0 to 5 nm results in prolongation of rise edge (the onset time of luminescence time trace to reach the highest value) of ~540 nm UC emission ($^4S_{3/2}$ energy state) from 200 to 564 μs. Similar result could also be observed for the red UC emission ($^4F_{9/2}$ excited state, i.e. ~650 nm UC emission), which prolonged from 370 to 765 μs. In addition, the influence of Yb^{3+} dopant concertation on energy migration dynamics has also been studied. In another YbEr@Yb@Nd DISS nanostructure (short for $NaYF_4$: 20% Yb, 2% Er@$NaLuF_4$: *x* Yb@$NaYF_4$:20%Nd), we find that the migration time will decrease as the Yb^{3+} dopant concertation increases (*x* value varies from 10% to 40%, the according rise edges decrease from 570 to 415 μs). The reason is as follows: increasing Yb^{3+} dopant concentration in the middle layer results in two opposite effects. (i) It speeds up the $Yb^{3+}\rightarrow Yb^{3+}$ energy migration rate. (ii) It decreases the Yb^{3+}-Yb^{3+} distance, leading to increasing the number of Yb^{3+}-Yb^{3+} plies in a fixed distance in space. As indicated in our previous work [4], the simulation and experimental results all revealed that: the effect of rapid increased energy migration rate will cover the effect of smooth increased Yb^{3+}-Yb^{3+} plies, thus leading to a shortened rise edge with the Yb^{3+} dopant concertation increasing.

Next we turn to tune the decay edge of time-resolved UC

emission in a wide range, which is not only required for practical applications [26], but also very important for an in-depth understanding of the UC mechanism [2,27]. Up to now, modulation approach was almost exclusively achieved by changing the depopulation rate of the activator emitting energy level, such as surface modification, Ln^{3+} dopant concentration manipulation, plasmonic effect and introducing extra energy transfer channels. All these tuning approaches face the following problems: limited adjustable range and/or reducing the UC efficiency and/or harmful to stability of the systems. Here, we propose a novel strategy, i.e. utilizing the energy migration process in DISS nanostructures characterized with partly overlapped sensitizer and activator regions [4].

As shown in Figure 7(a), taking the YbEr@Yb core/active shell nanostructure (short for $NaYF_4$: 20% Yb, 2% Er@$NaYF_4$: 20% Yb) as an example. The UC processes in this DISS nanostructure can be roughly divided into three parts. In part I, Yb^{3+} and Er^{3+} are co-doped, therefore its UC emission dynamics presents as a relatively sharp rise edge due to the minimal energy migration time. On the contrary, for parts II and III, the spatially separated Yb^{3+} and Er^{3+} require the excitation energy to migrate with more time to achieve UC emission, which plays as a continuous filling process of the UC emission energy levels. Notably, the UC emission time trace is a profile of contributions of all the three parts, thus it makes the decay longer than any of the individual parts. As a result, the UC emission (~540 nm) decay lifetime (the required time for transient emission intensity to decay from its maximum value to its 1/e value) could be tuned over a wide range from 139 to 648 μs by varying the active shell thickness from 0 to 15 nm. On the contrast, without the assistance of energy migration process in shell, the YbEr@Y core/inert shell structures (short for $NaYF_4$: 20% Yb, 2% Er@$NaYF_4$, as shown in Figure 7(b), (c)), offer a relatively narrow tuning range (from 139 to 330 μs) via the pure effect of eliminating the surface quenching sites. Significance of these results is that (i) it breaks through the tuning-range limitation of the traditional co-doping systems, (ii) it guides us to reconsider the relationship between UC efficiency and decay lifetime. Based on the empirical views developed from sensitizer-activator co-doping systems, on the premise of constant radiative relaxation rate, the longer UC emission decay lifetime is always related to a higher UC efficiency due to the reduction of nonradiative relaxation rate. This view is, however, not always valid to DISS nanostructures. As indicated in our previous report [4], compared with YbEr@Y nanostructure, the YbEr@Yb DISS nanostructure exhibits a relatively long decay lifetime but a relatively low UC efficiency when the shell thickness is over 6 nm. This "abnormal" phenomenon can be explained by (1) the energy migration effect of the active shell (prolonging the decay lifetime) and (2) the efficient energy back-transfer from core to active shell (decreasing the UC efficiency), which also well predicted by the Monte Carlo simulations model. As labeled in Table 3, compared with the YbEr@Y nanostructure, despite the YbEr@Yb DISS nanostructure owns several times higher absoprtion ability of the pump light, unfortunately, ~70% absorpted energy will be consumed by the surface quenching sites due to the harmful energy back-transfer effect. Therefore, its UC emission intensity is much lower than that of the YbEr@Y nanostructure.

4 Summary and future perspective

In summary, we have reviewed the recent processes of the investigaton of UC luminescence dynamics. In particular, the long standing puzzle of the intimate link between excitation energy migration and UC luminescence dynamics is unraveled. Utilizing the accumulative effect of multiple-step random walks of the excitation migration, we propose and demonstrate a convenient and effective approach for tailoring UC dynamics (either the rise or decay edge) via tuning the excitation energy migration paths in well-designed "dopant ions spatially separated" nanostructures.

In our opinion, further development of UC luminescence dynamics investigation can be focused on the following aspects: (i) optimizing the simulation model so that it can be

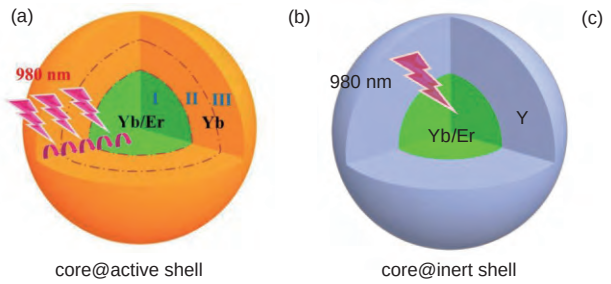

(c)

Sample	Decay lifetime (μs)	
	Active shell	Inert shell
Bare core	139	139
3 nm shell	220	310
6 nm shell	324	320
10 nm shell	470	315
15 nm shell	648	330

Figure 7 (Color online) Schematic illumination of the energy transfer/migration processes in the (a) YbEr@Yb core/active shell DISS nanostructure and (b) YbEr@Y core/inert shell nanostructure. (c) The shell thicknesses depedent ~540 nm UC emission decay lifetime of the core/active shell and core/inert shell nanostructures.

Table 3 The simulation results for YbEr@Y core/inert shell and YbEr@Yb core/active shell nanoparticles (core: 20 nm, shell thickness: 6 nm, simulation time period: 2 s)

Parameters	Inert shell	Active shell
Absorbed photons	166505	734445
Quenched by surface	0	517450
Recombined on the S_1 state	130249	173026
Recombined on the A_1 state	31132	41229
Recombined on the A_2 state	2515	1320
UC emission photons	1260	665
UC efficiency	0.75%	0.00091
Excited states number	~ 85	~110

applied to more complex systems (such as considering more complex energy levels or anisotropic energy migration in non-simple cubic crystal structure); (ii) utilizing theoretical model to guide the experiment, which could be one of the most promising approaches to design highly efficient UC material.

This work was supported by the European Union MSCA-ITN-ETN Action Program, Image-Guided Surgery and Personalised Postoperative Immunotherapy to Improving Cancer Outcome (ISPIC) (Grant No. 675743), the Netherlands Organisation for Scientific Research in the framework of the Fund New Chemical Innovation (Grant No. 731.015.206), the European COST Action (Grant No. CM1403), the Joint Research Program between CAS of China and the Royal Netherlands Academy of Arts and Sciences (KNAW) and Innovation Project of State Key Laboratory of Luminescence and Applications of China.

1 Chen G, Qiu H, Prasad P N, et al. Upconversion nanoparticles: Design, nanochemistry, and applications in theranostics. Chem Rev, 2014, 114: 5161–5214
2 Zheng W, Huang P, Tu D, et al. Lanthanide-doped upconversion nanobioprobes: Electronic structures, optical properties, and biodetection. Chem Soc Rev, 2015, 44: 1379–1415
3 Boyer J C, van Veggel F C J M. Absolute quantum yield measurements of colloidal $NaYF_4$: Er^{3+}, Yb^{3+} upconverting nanoparticles. Nanoscale, 2010, 2: 1417–1419
4 Zuo J, Sun D, Tu L, et al. Precisely tailoring upconversion dynamics via energy migration in core-shell nanostructures. Angew Chem Int Ed, 2018, 57: 3054–3058
5 Inokuti M, Hirayama F. Influence of energy transfer by the exchange mechanism on donor luminescence. J Chem Phys, 1965, 43: 1978–1989
6 Chan E M, Han G, Goldberg J D, et al. Combinatorial discovery of lanthanide-doped nanocrystals with spectrally pure upconverted emission. Nano Lett, 2012, 12: 3839–3845
7 Burshtei. A. Jump mechanism of energy-transfer. Zhurnal Eksperimentalnoi Teor Fiz, 1972, 62: 1695
8 Yokota M, Tanimoto O. Effects of diffusion on energy transfer by resonance. J Phys Soc Jpn, 1967, 22: 779–784
9 Grant W J C. Role of rate equations in the theory of luminescent energy transfer. Phys Rev B, 1971, 4: 648–663
10 Liu H, Huang K, Valiev R R, et al. Photon upconversion kinetic nanosystems and their optical response. Laser Photonics Rev, 2018, 12: 1700144
11 Tu L, Liu X, Wu F, et al. Excitation energy migration dynamics in upconversion nanomaterials. Chem Soc Rev, 2015, 44: 1331–1345
12 Wang F, Deng R, Wang J, et al. Tuning upconversion through energy migration in core-shell nanoparticles. Nat Mater, 2011, 10: 968–973
13 Su Q, Han S, Xie X, et al. The effect of surface coating on energy migration-mediated upconversion. J Am Chem Soc, 2012, 134: 20849–20857
14 Zhong Y, Tian G, Gu Z, et al. Elimination of photon quenching by a transition layer to fabricate a quenching-shield sandwich structure for 800 nm excited upconversion luminescence of Nd^{3+}-sensitized nanoparticles. Adv Mater, 2014, 26: 2831–2837
15 Vetrone F, Naccache R, Mahalingam V, et al. The active-core/active-shell approach: A strategy to enhance the upconversion luminescence in lanthanide-doped nanoparticles. Adv Funct Mater, 2009, 19: 2924–2929
16 Zhong Y, Rostami I, Wang Z, et al. Energy migration engineering of bright rare-earth upconversion nanoparticles for excitation by light-emitting diodes. Adv Mater, 2015, 27: 6418–6422
17 Wang J, Deng R, MacDonald M A, et al. Enhancing multiphoton upconversion through energy clustering at sublattice level. Nat Mater, 2014, 13: 157–162
18 Deng R, Wang J, Chen R, et al. Enabling Förster resonance energy transfer from large nanocrystals through energy migration. J Am Chem Soc, 2016, 138: 15972–15979
19 Fischer S, Bronstein N D, Swabeck J K, et al. Precise tuning of surface quenching for luminescence enhancement in core-shell lanthanide-doped nanocrystals. Nano Lett, 2016, 16: 7241–7247
20 Hossan M Y, Hor A, Luu Q A, et al. Explaining the nanoscale effect in the upconversion dynamics of β-$NaYF_4$:Yb^{3+} , Er^{3+} core and core-shell nanocrystals. J Phys Chem C, 2017, 121: 16592–16606
21 Anderson R B, Smith S J, May P S, et al. Revisiting the NIR-to-Visible upconversion mechanism in β-$NaYF_4$:Yb^{3+}, Er^{3+}. J Phys Chem Lett, 2014, 5: 36–42
22 Chen X, Jin L, Kong W, et al. Confining energy migration in upconversion nanoparticles towards deep ultraviolet lasing. Nat Commun, 2016, 7: 10304
23 Wang Y F, Liu G Y, Sun L D, et al. Nd^{3+}-sensitized upconversion nanophosphors: Efficient*in vivo* bioimaging probes with minimized heating effect. ACS Nano, 2013, 7: 7200–7206
24 Pollnau M, Gamelin D R, Lüthi S R, et al. Power dependence of upconversion luminescence in lanthanide and transition-metal-ion systems. Phys Rev B, 2000, 61: 3337–3346
25 Wang D, Xue B, Kong X, et al. 808 nm driven Nd^{3+}-sensitized upconversion nanostructures for photodynamic therapy and simultaneous fluorescence imaging. Nanoscale, 2015, 7: 190–197
26 Lu Y, Zhao J, Zhang R, et al. Tunable lifetime multiplexing using luminescent nanocrystals. Nat Photonics, 2014, 8: 33–37
27 Auzel F. Upconversion and anti-stokes processes with f and d ions in solids. Chem Rev, 2004, 104: 139–174